# BCL-2 modifying factor (BMF) is a central regulator of anoikis in human intestinal epithelial cells

Hausmann, M ; Leucht, K ; Ploner, C ; Kiessling, S ; Villunger, A ; Becker, H ; Hofmann, C ; Falk, W ; Krebs, M ; Kellermeier, S ; Fried, M ; Schölmerich, J ; Obermeier, F ; Rogler, G

Abstract: BCL-2 modifying factor (BMF) is a sentinel considered to register damage at the cytoskeleton and to convey a death signal to B-cell lymphoma 2. B-cell lymphoma 2 is neutralized by BMF and thereby facilitates cytochrome C release from mitochondria. We investigated the role of BMF for intestinal epithelial cell (IEC) homeostasis. Acute colitis was induced in Bmf-deficient mice (Bmf(-/-)) with dextran sulfate sodium. Colonic crypt length in Bmf(-/-) mice was significantly increased as compared with WT mice. Dextran sulfate sodium induced less signs of colitis in Bmf(-/-) mice, as weight loss was reduced compared with the WT. Primary human IEC exhibited increased BMF in the extrusion zone. Quantitative PCR showed a significant up-regulation of BMF expression after initiation of anoikis in primary human IEC. BMF was found on mitochondria during anoikis, as demonstrated by Western blot analysis. RNAi mediated knockdown of BMF reduced the number of apoptotic cells and led to reduced caspase 3 activity. A significant increase in phospho-AKT was determined after RNAi treatment. BMF knockdown supports survival of IEC. BMF is induced in human IEC by the loss of cell attachment and is likely to play an important role in the regulation of IEC survival.

DOI: https://doi.org/10.1074/jbc.M111.265322

# BCL-2 MODIFYING FACTOR (BMF) IS A CENTRAL REGULATOR OF ANOIKIS IN HUMAN INTESTINAL EPITHELIAL CELLS

**Martin Hausmann[1], Katharina Leucht[1], Christian Ploner[2], Stephan Kiessling[3], Andreas Villunger[3], Helen Becker[1], Claudia Hofmann[4], Werner Falk[4], Michaela Krebs[1], Silvia Kellermeier[1], Michael Fried[1], Jürgen Schölmerich[4], Florian Obermeier[4], Gerhard Rogler[1]**

Division of Gastroenterology and Hepatology, Department of Internal Medicine, University Hospital of Zürich, 8091 Zürich, Switzerland [1], Division of Molecular Pathophysiology, Biocenter, Medical University Innsbruck, Austria [2], Division of Developmental Immunology, Biocenter, Medical University Innsbruck, Austria [3], Department of Internal Medicine I, University of Regensburg, Germany[4]

Running head: BMF is a central regulator of intestinal epithelial cell apoptosis

Address correspondence to: Martin Hausmann, PhD, Division of Gastroenterology and Hepatology, Department of Internal Medicine, University Hospital of Zürich, Raemistasse 100, 8091 Zurich, Switzerland, E-mail: martin.hausmann@usz.ch

**BCL-2 modifying factor (BMF) is a sentinel considered to register damage at the cytoskeleton and to convey a death signal to B-cell lymphoma (BCL)-2. BCL-2 is neutralised by BMF and thereby facilitates cytochrome C release from mitochondria. We investigated the role of BMF for intestinal epithelial cell (IEC) homeostasis. Acute colitis was induced in *Bmf* deficient mice (*Bmf*$^{-/-}$) with dextran sulfate sodium (DSS). Colonic crypt length in *Bmf*$^{-/-}$ mice was significantly increased as compared to wildtype (WT) mice. DSS induced less signs of colitis in *Bmf*$^{-/-}$ mice as weight loss was reduced compared to WT. Primary human IEC exhibited increased BMF in the extrusion zone. qPCR showed a significant upregulation of *BMF* expression after initiation of anoikis in primary human IEC. BMF was found on mitochondria during anoikis as demonstrated by Western. RNAi mediated knock down of *BMF* reduced the number of apoptotic cells and led to reduced caspase-3 activity. A significant increase in pAkt was determined after RNAi treatment. *BMF* knock down supports survival of IEC. BMF is induced in human IEC by the loss of cell attachment and is likely to play an important role in the regulation of IEC survival.**

Intestinal epithelial cells (IEC) are generated from stem cells at the base of the crypt and migrate on the underlying basement membrane towards the intestinal lumen in 3 to 5 days, where apoptosis is initiated and cells finally lose anchorage and are shed into the lumen (1-4). IEC undergo apoptosis when they lose their contact with the extracellular matrix (5), a phenomenon termed “anoikis” (6). This special form of cell death is an important mechanism terminating the physiological life cycle of IEC (7-12). In contrast, carcinoma cells are resistant to anoikis, which is one of the pre-requisites for cancer development (13-14).

The activation of the apoptotic cascade leads to the cleavage of various structurally and functionally essential intracellular substrate proteins (15). We recently demonstrated that the preservation of cell-cell contacts and cell-matrix anchorage maintains both intercellular attachment and crypt structure diminishing initiation of the apoptotic cascade (16). Members of the B-cell lymphoma (BCL)-2 family of proteins decide over a cell’s life or death. BCL-2 is located on the outer mitochondrial membrane and prevents the release of cytochrome C from the mitochondrion. BCL-2 can interact with BMF (BCL-2-modifying factor), a member of the pro-apoptotic BH3-only protein subgroup of the BCL-2 family. BMF was first described in 2001 (17) and initially discussed to transduce death signals caused by different forms of cell stress such as UV-irradiation or loss of contact to the extracellular matrix, i.e. anoikis, or inhibition of the CAP-dependent translation machinery (18). However, studies in different cell types from *Bmf*-deficient mice suggested redundancy with other BH3-only proteins during most of these cell death processes (19). BMF interacts intracellularly with the dynein light chain 2 (DLC2), a component of the myosin V motor complex. By this BMF can be separated from BCL-2. Some stress stimuli have been reported to induce the release of BMF from the complex and its translocation to mitochondria (17,20). Mutations in light-chain-

binding domain of BMF enhance the death promoting activity of this protein in cell culture (17). BMF (as well as BAD, NOXA and PUMA) is also considered to act as sensitizer, which binds pro-survival BCL-2 protein to displace activator BH3-only proteins (i.e. BID or BCL-2-interacting mediator of cell death (BIM)) from BCL-2 to promote cell death (21). The interaction of BMF with BCL-2 on the mitochondrial surface neutralizes the anti-apoptotic action of BCL-2. Activator BH3-only proteins bind BAX and BAK, essential for mitochondrial apoptosis by forming pores in the mitochondrial membrane, and induce the release of cytochrome C finally triggering apoptosis. Alternatively, BMF may contribute to the neutralization of pro-survival proteins present in a cell, considered equally sufficient to induce apoptosis (22).

BMF transduces death signals not only after release from the actin cytoskeleton, but also by activation of transcription. *BMF* transcription is induced by transforming growth factor-β (TGFβ)-driven apoptosis in a number of cell types (23). TGFβ-induced autophagy potentiates the induction of the pro-apoptotic proteins BMF and BIM by the stress-responsive transcription factor CHOP upon growth factor withdrawal (24). Once BCL-2 is neutralized and cytochrome C is released out of the mitochondrion the so-called ”apoptosome“ is built, inducing a proteolytic cascade of caspases (25-29). During anoikis of human IEC, caspases-2 and -9 are reportedly involved in the initiation of anoikis and activate downstream effector caspases-7, -3 and -6 (30). This results in a sequential cleavage of focal adhesion kinase (FAK) by caspase-3 and caspase-6 (31) and culminates in characteristic apoptotic morphological changes.

Together, this suggests that BMF may be critical for epithelial cell homeostasis. We investigated the role of BMF for cell death of IEC in mice under inflammatory conditions as well as in isolated primary human IEC.

## Experimental Procedures

*Patients*- Primary human IEC were obtained from surgical specimens from intestinal mucosa of 62 patients undergoing surgery in the large or small bowel (> 10 cm distance from the tumor for carcinoma patients, supplemental table 1). 34 were male and 28 were female. Patients were between 17 and 89 (mean 51 ± 17) years of age. This study was approved by the Ethics Committees of the University of Regensburg and the University of Zurich and performed according to the declaration of Helsinki.

*Induction and treatment of dextran sulfate sodium (DSS) colitis*- Male C57BL/6-*Bmf*$^{tm1.1Anvi}$ (*Bmf*$^{-/-}$) mice were backcrossed for at least 12 generations (19). Mice weighing 25-32 g were used for the experiments and housed in individually ventilated cages. Acute colitis was induced as described previously (32). During induction of acute colitis mice received either 3.5 % DSS in drinking water or drinking water alone over eight days. Animals were provided unlimited access to food and water throughout the experiment (ad libitum). Mice were killed on day eight. From the distal third of the colon, 1 cm of colonic tissue was removed and used for histological analysis, as described previously (32-33).

*Cell lines, IEC isolation and induction of anoikis*- Cells were grown in RPMI 1640 (Bio Whitaker, Verviers, Belgium) supplemented with 10 % fetal calf serum (FCS), 100 U/ml penicillin, 100 µg/ml streptomycin and 2 mM L-glutamine (GIBCO, Invitrogen cell culture, Vienna, Austria) at 37ºC, 5 % $CO_2$. HEK293T packaging cells for lentivirus production were grown in DMEM (BioWitthaker) containing 10 % FCS, 100 U/ml penicillin, 100 µg/ml streptomycin and 2 mM L-glutamine (GIBCO).

IEC were isolated as described in (34) and in the supplement. For induction of anoikis, IEC were liberated from crypts by agitation at 37°C on a whip-shaker.

*Antibodies*- Primary antibodies: Rat anti-BMF IgG2a (#9G10, Alexis, Lörrach, Germany, 1:500), rabbit anti-human BMF (#ab59906, abcam, 1:100), rabbit anti-cleaved caspase-3 (Asp175, #9661, Cell signalling Technology, Beverly, MA, 1:3000), mouse anti-caspase-3 IgG2a (#610322, BD, Lexington, KY, 1:3000), rabbit anti-pAKT (#9271, Cell Signaling, 1:1000), mouse anti-caspase-6 IgG1 (#556581, BD, 1:1000), rabbit anti-cleaved caspase-6 (#9761, Cell Signaling, 1:1000), mouse anti-caspase-7 IgG1 (#9494, Cell Signaling, 1:1000), mouse anti-human cytochrome C oxidase; mitochondria complex (COX) IV (#MS408, Acris, 1:2000) and mouse

anti-β-actin IgG1 (#sc8432, Santa Cruz, 1:10 000).

Isotype controls: rat IgG2a (#ab18450, Abcam, Cambridge, UK), rabbit and mouse IgG (sc-2027 and sc-2025, Santa Cruz). Secondary antibodies: Alexa Fluor 488 goat anti-rat IgG (#A11006, Molecular Probes OR, USA, 1:300), goat anti-rat IgG, goat anti-rabbit IgG and goat-anti-mouse IgG (IgG-HRP, sc-2006, sc-2004, sc-2005, Santa Cruz, 1:5000)

*Digitonin-based subcellular fractionation and Western*- For isolation of mitochondria, IEC ($3 \times 10^7$) were washed in ice cold PBS. Cells were digitonin-permeabilized in 1 ml cytosolic extraction buffer (200 µg/ml digitonin, #D141, Sigma, and a complete mini tablet, #04 693 124 001, Roche, Mannheim, Germany, in 250 mM sucrose, 70 mM KCl, 137 mM NaCl, 4.3 mM $Na_2HPO_4$, 1.4 mM $KH_2PO_4$, pH 7.2). Plasma membrane permeabilization of cells was confirmed by staining in a trypan blue solution. Cells were centrifuged at 1000 g for 5 min at 4°C. The supernatant (cytosolic fraction) was saved and the pellets were solubilized in the same volume of mitochondrial lysis buffer (50 mM Tris, 150 mM NaCl, 2 mM EDTA, 2 mM EGTA, 0.2 % Triton X-100, 0.3 % NP-40 and a complete mini tablet, pH 7.4), followed by pelleting at 10 000 g for 10 min at 4°C. The supernatant was collected as mitochondrial fraction. Western was performed as described in the supplement and in (16).

*Virus generation and Transfection*- Vector cloning and infections were performed as described in the supplement and in (35). Human mucosa for viral transduction was transferred immediately after surgery in the viral supernatant. Isolation of intestinal crypts was performed in lentivirus-containing media. Isolation was finished within a time period of 1.5 hours. Crypts were then kept on collagen-coated transwells at 37°C, 5 % $CO_2$ in lentivirus-containing media. After 24 hours on transwells, IEC were isolated. Including the transport of the resection from the department of surgery IEC were kept in virus containing media for 25.5 hours. After 25.5 hours, IEC were isolated.

*Statistical analysis*- Real time PCR data were calculated from triplicates. Statistical analysis was performed using the Mann-Whitney rank sum test. One-Way ANOVA test was used for body weight, colon length and real time PCR if four groups were compared. Mann-Whitney rank sum test was used for crypt length, real time PCR if two groups were compared, Western blot. Data are expressed as mean ± S.D. Differences were considered significant at $p < 0.05$ (*), highly significant at $p < 0.01$ (**) and very highly significant at $p < 0.001$ (***). For statistical analysis of Westerns, luminescence signals were determined by densitometry and quantified with the OptiQuant software (Packard Instrument, Meriden, CT, USA).

## Results

*Crypt structures are protected in Bmf$^{-/-}$ mice upon DSS-colitis.* We focused on the involvement of BMF in inflammatory responses and its property to induce apoptosis in IEC. Colonic crypt lengths for *Bmf*$^{-/-}$ mice were significantly increased compared to wildtype ($156.9 \pm 32.0$ µm, $n = 99$ and $139.8 \pm 22.4$ µm, $n = 96$, calculated from sections of 5 mice respectively, $p < 0.05$, figure 1A - C). A hydrometrocolpos was described in female *Bmf*$^{-/-}$ mice. Confirmative to this, we observed an enlarged uterovaginal tract in *Bmf*$^{-/-}$ mice.

We used the DSS colitis mouse model to determine BMF-dependence of mucosal inflammation. During induction of acute colitis mice received 3.5 % DSS in drinking water ($n = 10$) or drinking water alone ($n = 10$) over eight days. Water consumption was not reduced in mice treated with DSS (126 ml for *Bmf*$^{-/-}$ mice with DSS, 121 ml for *Bmf*$^{-/-}$ mice with water, 119 ml for wildtype with DSS and 122 ml for wildtype with water, $n = 5$ each). Upon DSS, weight loss of *Bmf*$^{-/-}$ mice was significantly decreased from day five to eight compared to wildtype mice (figure 1D). Upon DSS, no blood was visible on the anus of *Bmf*$^{-/-}$ mice, whereas two wildtype mice displayed blood on the anus from day four to day eight and four wildtype mice displayed blood on the anus from day five to day eight. Upon DSS, no aggressive behavior was observed in cages with *Bmf*$^{-/-}$ mice, whereas wildtype mice showed aggressive behavior from day four to day eight. Induction of colitis was followed by a typical and significant reduction of colon length (supplemental figure 1A and B). *Bmf*$^{-/-}$ mice with and without colitis showed an increased colon length.

Previous experimental evidence reported impaired cell death in lymphocytes in the absence of BMF, but no significant differences between wildtype and *Bmf*$^{-/-}$ mice IEC undergoing cell death *in vitro* were noted (19). Consistently, we failed to observe differences in the histological score between *Bmf*$^{-/-}$ and wildtype mice receiving water ($0.9 \pm 0.4$ for *Bmf*$^{-/-}$ mice and $1.3 \pm 0.8$ for wildtype mice, $n = 5$ each). The histological score for *Bmf*$^{-/-}$ mice and wildtype mice receiving DSS was also not significantly altered ($7.6 \pm 0.4$ and $7.4 \pm 0.7$ respectively).

To locate apoptotic cells in colonic tissue we performed TUNEL analysis. Cleavage of genomic DNA during apoptosis was found in an expected dimension. Apoptosis was not uniform along the crypt-villus axis. In crypts, positively stained cells were preferentially detected apically, close to the lumen. Confirmative to previous findings based on FACS analysis, TUNEL staining revealed no decrease in apoptosis from colonic IEC lacking BMF *in situ* (supplemental figure 1C - F). Mucosa from mice suffering from DSS colitis showed an extensive epithelial damage and both infiltration and thickening of the mucosa. In wildtype and *Bmf*$^{-/-}$ mice receiving DSS, crypt morphology was absent and goblet cells were lost. To detect remaining IEC, EpCAM staining was performed. $45 \pm 37$ % of IEC remained as a layer on the thickened mucosa of the distal end of the colon in *Bmf*$^{-/-}$ mice upon DSS compared to $34 \pm 33$ % in DSS-treated wildtype mice (supplemental figure 1G and H).

*BMF expression is induced along the human crypt-villus axis.* IEC mature along the crypt-villus axis. Maturation is reflected in both changes of gene expression and transition from an epithelial stem cell, firmly embedded in the crypt, to a cell intrinsically prone to anoikis and prepared to be detached. BMF on mitochondria results in cytochrome C release from mitochondria and activation of the caspase cascade leading to apoptosis. Immunohistochemistry (IHC) was performed to localize BMF in human colonic sections. IEC exhibited intense staining in the extrusion zone where cells are expected to be shed. Brown staining was found in IEC in human mucosa (figure 2A - B). IEC were isolated from patients by three successive agitation procedures. Single cells were separated from whole crypts and the relative amount of *BMF* cDNA was calculated by means of real time PCR. Data from crypts were set to 1. *BMF* mRNA in single IEC from patients without inflammatory bowel disease (IBD) was $2.2 \pm 2$-fold increased compared to crypts (figure 2D). *BMF* mRNA in single cells from patients with IBD was significantly increased ($4.8 \pm 1.5$-fold, Mann-Whitney rank sum test, $p < 0.05$) compared to crypts. The same trend was found for *PUMA* and *BID* without reaching statistical significance (supplemental figure 2A and B). Human IEC are fractionated during the isolation procedure according to their capacity of staying attached to the colonic mucosa. *BMF* mRNA is downregulated in IEC obtained in second and third fractions (figure

2E). Data from the first IEC fraction of each surgical specimen were set to 100 %. Significant differences were determined between the first and the second crypt fraction (-66 ± 32 %) and the first and the third fraction of single cells (-29 ± 3 %, ANOVA multiple variance analysis, $p < 0.05$).

*BMF is upregulated and found on mitochondria during anoikis.* Anoikis is the inevitable end of the IEC life cycle. Anoikis is also inducible by disconnecting cell-cell and cell-matrix contacts as described in materials and methods. Real time PCR was performed from freshly isolated human IEC and detached IEC, 2 h after *ex-vivo* isolation from 19 surgical specimens. The initiation of anoikis is followed by a significant upregulation of *BMF* mRNA ($p < 0.05$, figure 3A). Significant upregulation was found for *PUMA* (supplemental figure 3, Mann-Whitney Rank Sum Test. $P < 0.05$).

We examined BMF level in mitochondria from human IEC after the induction of anoikis. Cells from the last of the three successive agitation procedures were used. Mitochondria were prepared from freshly isolated IEC and from IEC incubated without matrix contact for 2 h after *ex-vivo* isolation. Figure 3B shows BMF in the mitochondrial fraction 2 h after induction of anoikis (23 and 25 kDa, upper box). This could be due to higher expression levels. Immediately after isolation of IEC, BMF was barely visible in the mitochondrial fraction.

*Knock down of BMF reduces anoikis in human IEC.* Anoikis is initiated following neutralization of the anti-apoptotic BCL-2 proteins through association of BMF and/or other BH3-only proteins. HEK293T were transfected for virus assembly. Development of virus in supernatants and efficient transduction was confirmed (supplemental material, figure 4A - E). Including the transport of the resection from the department of surgery, isolation of crypts and incubation on transwells IEC were kept in virus containing media for 25.5 hours. Efficient infection of human crypts, kept on collagen coated transwells, was confirmed by fluorescence microscopy (figure 4A). Viability of IEC was confirmed by trypan blue staining (figure 4B). Knock down of *BMF* in IEC was confirmed by determining BMF with Western (figure 4C). Efficient downregulation of *BMF* mRNA in infected IEC was confirmed by real time PCR. Mock-infected IEC had a *BMF* / *GAPDH* ratio of 8.0 ± 5.8 (n = 3) and virus-infected cells had a *BMF / GAPDH* ratio of 0.2 ± 0.2 (n = 3). We investigated, whether knock down of *BMF* by the lentiviral system is able to delay anoikis in human IEC. For fluorescence microscopy cells were mounted with medium containing DAPI. Freshly isolated human IEC displayed round shaped nuclei revealing no indication of anoikis (figure 4D). To induce anoikis single IEC were liberated from isolated crypts by agitation at 37°C on a whip-shaker in media including EDTA for 2 h and harvested by centrifugation. Fluorescence microscopy showed cells with a disintegrated nuclei pattern, a clear sign of ongoing execution of anoikis (figure 4E). No round shaped nuclei were found. Figure 4F shows cells with *BMF* knock down 2 h after induction of anoikis. The number of apoptotic nuclei was lower than in the experiments without knock down as a number of round shaped nuclei were found. These data show that *BMF* knock down in human IEC is capable of preserving cellular morphology.

*Knock down of BMF maintains phosphorylation of Akt and blocks activation of caspases.* Including the transport of the resection from the department of surgery, isolation of crypts and incubation on transwells IEC were kept in virus containing media for 25.5 hours. Phosphorylation of the important pro-survival signaling molecule AKT in human crypts, isolated within the first fraction of IEC, was determined by Western. AKT reportedly promotes cell survival by inhibiting anoikis via phosphorylation and inactivation of several proapoptotic targets including BAD and caspase-9 (16). Phosphorylation, and thereby activation, of the protein kinase AKT was detectable by Western at 60 kDa (pAKT). After *BMF* knock down AKT was found in an activated state in IEC, kept on collagen-coated transwells for 24 hours while pAKT levels in dying mock-infected cells were clearly lower (figure 5A). This indicates that survival pathways can be maintained efficiently when cells are protected from apoptosis due to lack of BMF. Following the studies on fragmentation of the nuclei, we addressed the impact of *BMF* knock down on the activation of caspases, as execution of the caspase cascade initiates degradation of DNA. To investigate the effect of *BMF* knock down,

caspase-3 activation in response to induction of anoikis in whole crypts of human IEC with and without *BMF* knock down was determined by Western (figure 5B). Mock-treated IEC showed increased levels of active caspase-3, illustrating ongoing apoptosis.

Next, the lentiviral system was used to knock down *BMF* in whole resections of human colonic mucosa. Again, the incubation with virus-containing medium was immediately started after the surgery. In this experiment, after six hours of incubation in lentivirus containing medium, human IEC were isolated and kept for two hours on a whip-shaker for induction of anoikis. Cleavage of caspase-3 was determined in single cells from the first agitation step (figure 5C). IEC liberated from the basal lamina showed significantly higher levels of activated caspase-3 after mock infection compared to cells with *BMF* knock down ($n = 6$, Mann-Whitney rank sum test was performed, $p < 0.05$). This indicates decreased activation of death signals after *BMF* knock down.

Cleavage of caspase-6 and -7 was determined in lysates from cells collected after the first agitation step (figure 5D). Here, IEC were again kept in virus containing media for 25.5 hours. Western for inactive procaspase-6 (35 kDa) and procaspase-7 (35 kDa) demonstrated that both proteases were activated more effectively in the mock infected group. Next, we performed Western for activated caspase-3 in IEC of the first, second and third agitation steps with and without *BMF* knock down (figure 5E). Treatment with RNAi for *BMF* knock down led to lower amounts of active caspase-3. Taken together, these experiments demonstrate that activation of caspases is delayed by *BMF* knock down.

## Discussion

In the present study, we show that down-regulation of BMF suppresses anoikis in primary human IEC *in vitro*. In a second attempt we used the DSS-colitis mouse model to determine BMF-dependence of mucosal inflammation. Upon DSS weight of *Bmf*$^{-/-}$ mice was significantly increased compared to wildtype. *Bmf*$^{-/-}$ mice with and without colitis showed an increased colon length. Crypt lengths for *Bmf*$^{-/-}$ mice receiving water were significantly increased compared to water-treated wildtype mice. A possible explanation for an increased colon and crypt length could be that the lifespan of IEC in *Bmf*$^{-/-}$ mice is longer than in wildtype mice. The proportion of apoptotic IEC compared to the number of total cells in a crypt could be lower in *Bmf*$^{-/-}$ mice, synonymic with a decreased apoptosis rate of IEC in *Bmf*$^{-/-}$ mice. A decreased apoptosis rate and unchanged number of dead cells in a crypt at the same time could contribute to elongation of crypts. This could be protective during onset of inflammation. The histological score for *Bmf*$^{-/-}$ mice and wildtype mice receiving either water or DSS, however, was not significantly altered at the end of the experiment. Both water-treated groups showed almost no signs of inflammation. Mice from both DSS treated groups were severely inflamed at the distal end of the colon. Differentiation between both groups was not possible with this parameter.

Human colonic IEC exhibited intense staining in the extrusion zone. Expression of *BMF* in IEC was confirmed by real time PCR. The technique utilized to isolate IEC requires several successive agitation procedures to discriminate discrete fractions. In consequence of the isolation procedure both single cells and whole crypts embedded more loosely in the mucosal architecture are supposed to be isolated earlier during the procedure. Adhesion of IEC to the basal lamina is not uniform along the crypt-villus axis. Molecules regulated between crypt and villus, like tenascin and cellular fibronectin, are able to modify cellular adhesion and play a role in IEC shedding (7,10). Experimental induction of anoikis in human IEC was followed by a significant upregulation of *BMF*. We showed that protein levels increase in the mitochondrial fraction upon induction of anoikis in human IEC *in vitro*. This could be due to higher expression levels or translocation. Detachment of IEC, the trigger of anoikis, is associated with *BMF* upregulation. Cell death is initiated following neutralization of BCL-2 or homologues through association of BMF. We performed knock down of *BMF* to determine if cell survival could be prolonged. Knock down of *BMF* is able to delay anoikis in human IEC as shown with several assays: Fluorescence microscopy revealed a preserved morphology of the nuclei in knock down experiments. Activation of the downstream effector caspases 3, 6 and 7 is decreased as determined by Western. The signaling molecule Akt remained in an active state, indicating that the corresponding survival pathways were

maintained. Caspase-3 was activated in all single IEC suspensions but the most prominent effect of *BMF* knock down was determined in the third agitation fraction. These experiments confirmed differences in successive IEC fractions and indicate that in the latter fraction BMF is decreased and anoikis is least advanced.

Similar to our experiments Schmelzle et al. investigated the role of BMF in mammary epithelial anoikis (36). In mammary epithelial cells anoikis is induced by detachment from the matrix as in assays performed in the study presented here with colonic IEC. Interestingly, mRNA levels of *BMF* are up-regulated during anoikis upon loss of matrix attachment. Down-regulation of *BMF* expression by RNAi mediated knock down is sufficient to prevent anoikis.

BIM, another pro-apoptotic BH3-only protein family member, also interacts with the pro-survival family member BCL-2. BIM is functionally required for anoikis and a knockdown of *BIM* also prevents cell death (36). BMF is sequestered to the myosin V motor complex (17) and BIM to microtubule complexes (37), both cytoskeleton-associated structures. Both seem to monitor cytoskeletal integrity. Both proteins counteract the apoptotic activity of pro-survival BCL-2 when vital processes are disturbed. Maturation of IEC along the crypt-villus axis might be defined by different aspects. The spatial arrangement of a cell within a crypt, the genetic programming during maturation (38), the preservation of cell-cell contacts and cell-matrix anchorage (16), cellular remodelling or the intracellular damage status of a cell might contribute to the fate of a cell. Inhibition of BMF seems to be a possible medication for epithelial lesions. But others reminded the possibility that deletion of BMF would allow survival of tumor cells deprived of matrix interactions outside their natural "niche" (36). BMF was suggested as putative tumor suppressor gene in epithelial solid tumors because it is located on chromosome 15q14 (39), a site frequently lost in metastatic colon cancer, and actively prevents formation of c-myc driven lymphomas.

In summary, this work describes the sequence of intracellular events during anoikis, a physiological form of apoptosis, in a population of primary human IEC. Our studies narrow down the initiating event leading to the activation of anoikis. Given the stronger expression of pro-survival BCL-2 family members in IEC at the base of the intestinal crypt (40) future studies are underway to delineate the reciprocal expression of its antagonist BMF and BIM.

## References


1. **Gavrieli, Y., Sherman, Y., and Ben-Sasson, S. A. (1992)** ***J Cell Biol*** **119, 493-501**
2. **Grossmann, J., Walther, K., Artinger, M., Rummele, P., Woenckhaus, M., and Scholmerich, J. (2002)** ***Am J Gastroenterol*** **97, 1421-1428**
3. **Potten, C. S., and Allen, T. D. (1977)** ***J Ultrastruct Res*** **60, 272-277**
4. **Strater, J., Koretz, K., Gunthert, A. R., and Moller, P. (1995)** ***Gut*** **37, 819-825**
5. **Grossmann, J. (2002)** ***Apoptosis*** **7, 247-260**
6. **Frisch, S. M., and Francis, H. (1994)** ***J Cell Biol*** **124, 619-626**
7. **Beaulieu, J. F. (1992)** ***J Cell Sci*** **102 ( Pt 3), 427-436**
8. **Gordon, J. I., and Hermiston, M. L. (1994)** ***Curr Opin Cell Biol*** **6, 795-803**
9. **Koretz, K., Schlag, P., Boumsell, L., and Moller, P. (1991)** ***Am J Pathol*** **138, 741-750**
10. **Probstmeier, R., Martini, R., and Schachner, M. (1990)** ***Development*** **109, 313-321**
11. **Riedl, S., Moller, P., Faissner, A., and Schlag, P. (1992)** ***Exs*** **61, 277-281**
12. **Zutter, M. M., and Santoro, S. A. (1990)** ***Am J Pathol*** **137, 113-120**
13. **Alnemri, E. S., Livingston, D. J., Nicholson, D. W., Salvesen, G., Thornberry, N. A., Wong, W. W., and Yuan, J. (1996)** ***Cell*** **87, 171**
14. **Cohen, G. M. (1997)** ***Biochem J*** **326 ( Pt 1), 1-16**
15. **Kemler, R. (1993)** ***Trends Genet*** **9, 317-321**
16. **Hofmann, C., Obermeier, F., Artinger, M., Hausmann, M., Falk, W., Schoelmerich, J., Rogler, G., and Grossmann, J. (2007)** ***Gastroenterology*** **132, 587-600**
17. **Puthalakath, H., Villunger, A., O'Reilly, L. A., Beaumont, J. G., Coultas, L., Cheney, R. E., Huang, D. C., and Strasser, A. (2001)** ***Science*** **293, 1829-1832**

18. **Grespi, F., Soratroi, C., Krumschnabel, G., Sohm, B., Ploner, C., Geley, S., Hengst, L., Hacker, G., and Villunger, A. (2010)** ***Cell Death Differ***
19. **Labi, V., Erlacher, M., Kiessling, S., Manzl, C., Frenzel, A., O'Reilly, L., Strasser, A., and Villunger, A. (2008)** ***J Exp Med*** **205, 641-655**
20. **Day, C. L., Puthalakath, H., Skea, G., Strasser, A., Barsukov, I., Lian, L. Y., Huang, D. C., and Hinds, M. G. (2004)** ***Biochem J*** **377, 597-605**
21. **Kutuk, O., and Letai, A. (2010)** ***Cell Death Differ***
22. **Pinon, J. D., Labi, V., Egle, A., and Villunger, A. (2008)** ***Oncogene*** **27 Suppl 1, S41-52**
23. **Ramjaun, A. R., Tomlinson, S., Eddaoudi, A., and Downward, J. (2007)** ***Oncogene*** **26, 970-981**
24. **Suzuki, H. I., Kiyono, K., and Miyazono, K. (2010)** ***Autophagy*** **6**
25. **Earnshaw, W. C., Martins, L. M., and Kaufmann, S. H. (1999)** ***Annu Rev Biochem*** **68, 383-424**
26. **Salvesen, G. S., and Dixit, V. M. (1997)** ***Cell*** **91, 443-446**
27. **Thornberry, N. A. (1998)** ***Chem Biol*** **5, R97-103**
28. **Grossmann, J., Walther, K., Artinger, M., Kiessling, S., and Scholmerich, J. (2001)** ***Cell Growth Differ*** **12, 147-155**
29. **Susin, S. A., Zamzami, N., Castedo, M., Daugas, E., Wang, H. G., Geley, S., Fassy, F., Reed, J. C., and Kroemer, G. (1997)** ***J Exp Med*** **186, 25-37**
30. **Gumbiner, B. M. (1996)** ***Cell*** **84, 345-357**
31. **Pece, S., and Gutkind, J. S. (2000)** ***J Biol Chem*** **275, 41227-41233**
32. **Obermeier, F., Kojouharoff, G., Hans, W., Scholmerich, J., Gross, V., and Falk, W. (1999)** ***Clin Exp Immunol*** **116, 238-245**
33. **Steidler, L., Hans, W., Schotte, L., Neirynck, S., Obermeier, F., Falk, W., Fiers, W., and Remaut, E. (2000)** ***Science*** **289, 1352-1355**
34. **Grossmann, J., Walther, K., Artinger, M., Kiessling, S., Steinkamp, M., Schmautz, W. K., Stadler, F., Bataille, F., Schultz, M., Scholmerich, J., and Rogler, G. (2003)** ***Eur J Cell Biol*** **82, 262-270**
35. **Ploner, C., Rainer, J., Niederegger, H., Eduardoff, M., Villunger, A., Geley, S., and Kofler, R. (2008)** ***Leukemia*** **22, 370-377**
36. **Schmelzle, T., Mailleux, A. A., Overholtzer, M., Carroll, J. S., Solimini, N. L., Lightcap, E. S., Veiby, O. P., and Brugge, J. S. (2007)** ***Proc Natl Acad Sci U S A*** **104, 3787-3792**
37. **Puthalakath, H., Huang, D. C., O'Reilly, L. A., King, S. M., and Strasser, A. (1999)** ***Mol Cell*** **3, 287-296**
38. **Mariadason, J. M., Nicholas, C., L'Italien, K. E., Zhuang, M., Smartt, H. J., Heerdt, B. G., Yang, W., Corner, G. A., Wilson, A. J., Klampfer, L., Arango, D., and Augenlicht, L. H. (2005)** ***Gastroenterology*** **128, 1081-1088**
39. **Wick, W., Petersen, I., Schmutzler, R. K., Wolfarth, B., Lenartz, D., Bierhoff, E., Hummerich, J., Muller, D. J., Stangl, A. P., Schramm, J., Wiestler, O. D., and von Deimling, A. (1996)** ***Oncogene*** **12, 973-978**
40. **Merritt, A. J., Potten, C. S., Watson, A. J., Loh, D. Y., Nakayama, K., Nakayama, K., and Hickman, J. A. (1995)** ***J Cell Sci*** **108 ( Pt 6), 2261-2271**

* This study was supported by grants from the Swiss National Science Foundation (SNF 31003A_127247 (to M. H.) and SNF 310030 120312 (to G. R.)), by the Deutsche Forschungsgemeinschaft (RO 1236/13–1), and the Bundesministerium für Bildung und Forschung Kompetenznetz Chronisch Entzündliche Darmerkrankungen. Support also received from the Zurich Center for IntegrativeHumanPhysiology (ZIHP, to M. H. and G. R.) and from the Swiss Inflammatory Bowel Disease Cohort Study (SIBDC, to G. R.).
□**S** The on-line version of this article (available at http://www.jbc.org) contains supplemental Figs. 1– 4, Table 1, and Materials and Methods.
1 To whom correspondence should be addressed: Division of Gastroenterology and Hepatology, Department of Internal Medicine, University Hospital of Zürich, Raemistrasse 100, 8091 Zürich, Switzerland. E-mail: martin.hausmann@usz.ch.
2 Supported by grant SFB-F021 from the Austrian Research Foundation.
3 Supported by grant OB135/10–1 from the German Research Foundation.
4 The abbreviations used are: IEC, intestinal epithelial cell(s); BCL, B-cell lymphoma; BMF, B-cell lymphoma-modifying factor; DSS, dextran sulfate sodium; BIM, BCL-2-interacting mediator of cell death.

## FIGURE LEGENDS

**Fig. 1.** Crypt length and body weight loss. Crypt lengths for (A) *Bmf*$^{-/-}$ mice receiving water and (B) wildtype mice receiving water. Section 0 - 1 cm from the distal end of the colon. (C) Normality test for crypt length in *Bmf*$^{-/-}$ mice and wildtype mice receiving water failed and Mann-Whitney rank sum test was performed. *Bmf*$^{-/-}$ mice showed a significant increased crypt length compared to wildtype mice. $P < 0.001$. (D) *Bmf*$^{-/-}$ mice (circles) and wildtype mice (triangles) received either DSS (filled) or water (empty). Bars represent mean ± s.d. One-Way ANOVA test was used. Body weight loss was significantly different for wildtype mice upon DSS compared to *Bmf*$^{-/-}$ mice upon DSS on day 5, 6, 7 and 8. Day 5 $P = 0.016$, day 6 $P = 0.008$, day 7 $P = 0.007$ and day 8 $P = 0.016$, n = 5 each. *Bmf*$^{-/-}$ mice showed a significant decreased body weight loss upon DSS and increased crypt length upon water.

**Fig. 2.** IHC for BMF on sections from human (A, B) large intestine and (C) small intestine. (A and B) Immunostaining of BMF on section from a Crohn's disease patients without inflammation. (C) Negative control without primary antibody. IHC revealed an expression gradient of BMF along the crypt-villus axis. DAB procedure. Original magnification (A and C) × 100, (B) × 200. (D) *BMF* is significantly increased in single IEC from IBD patients compared to crypts. (E) *BMF* is downregulated in IEC isolated in subsequent agitation procedures in both single cells and crypts. IEC were isolated by three successive agitation procedures and *BMF* expression was analyzed by real time PCR. One-Way ANOVA test was used. * $P < 0.05$.

**Fig. 3.** Initiation of anoikis is followed by upregulation of BMF. (A) Real time PCR of freshly isolated human IEC and human IEC 2 hours after *ex-vivo* isolation. Mann-Whitney rank sum test was performed. $P < 0.05$. n=19, ## = median. (B) Western of mitochondrial fractions of freshly isolated IEC and IEC 2 hours after *ex-vivo* isolation. A third BMF isoform seen in human IEC lysates was not detected in extracts from mouse spleen used as positive control. Western for COX IV (18 kDa) showed successful purification of mitochondria and demonstrates equal loading in the human IEC samples analyzed but, as expected was not detected in the mouse extract due to specificity to the human protein (lower box). Loss of cytochrome C (15 kDa) was only marginal 2 h after *ex-vivo* isolation (not shown). Data representative for three patients.

**Fig. 4.** Knock down of *BMF* in primary human IEC crypts. Including the transport of the resection from the department of surgery, isolation of crypts and incubation on transwells IEC were kept in virus containing media for 25.5 hours. (A) Fluorescent image of crypts infected with lentivirus. (B) Transmission light microscopic image of crypts, cultivated on collagen coated transwells and incubated with trypan blue. (C) Western and densitometry confirms downregulation of BMF. (D) Fluorescence microscopy of freshly isolated cells, (E) cells 2 hours after induction of anoikis and (F) cells with *BMF* knock down 2 hours after induction of anoikis. Knock down of *BMF* protects against condensation of chromatin. DAPI, x 630. Data representative for three patients.

**Fig. 5.** Knock down of *BMF* maintains active form of pro-survival factor AKT and inactive form of caspase-3 in primary human IEC. In (A, B, D and E) IEC were kept in virus containing media for 25.5 hours. (A) pAKT after induction of anoikis in whole crypts with and without *BMF* knock down. (B) Cleaved caspase-3 after induction of anoikis in whole crypts with (left) and without *BMF* knock down (right). Cleaved caspase-3 was normalized to caspase-3 proform. (C) After six hours of incubation in lentivirus containing medium cleaved caspase-3 after induction of anoikis in single cells with (left) and without *BMF* knock down (right), Mann-Whitney rank sum test was performed, $p < 0.05$, $n = 6$. Patients are not identical to those used in figure 5B. Cleaved caspase-3 was normalized to β-actin. (D) Knock down of *BMF* maintains inactivated caspases 6 and 7 in single cells. Data representative for three patients.

(E) Western for activated caspase-3 from IEC of the first, second and third agitation procedure with and without *BMF* knock down. IEC from 3 patients were isolated and anoikis was induced in both whole crypts (left) or in single cell suspension (right). Western for β-actin demonstrated equal loading of the samples. In the isolated, intact crypts, caspase-3 was activated independent of RNAi treatment in crypts from the first and second agitation procedure (4228 and 1853 density units respectively in the blot shown). Mann-Whitney rank sum test was performed. In both cases treatment

with RNAi led to significantly less active caspase-3 (53 ± 21 and 74 ± 39 % compared to untreated cells respectively, $n = 3$, $p < 0.05$). In cells from the third agitation procedure no activated caspase-3 was detectable. In isolated single IEC caspase-3 was activated without RNAi treatment in the suspension from all three agitation procedures (3275, 883 and 319 density units respectively in the blot shown). *BMF* knock down led to significantly reduced caspase-3 activity in single IEC from the first and the second agitation procedure (82 ± 57 and 70 ± 30 % compared to untreated cells respectively, $n = 3$, $p < 0.05$). In cells from the third agitation procedure no activated caspase-3 was detectable. Whole crypts and single cells were isolated by three successive agitation procedures. Data representative for six patients.

**Figure 1**

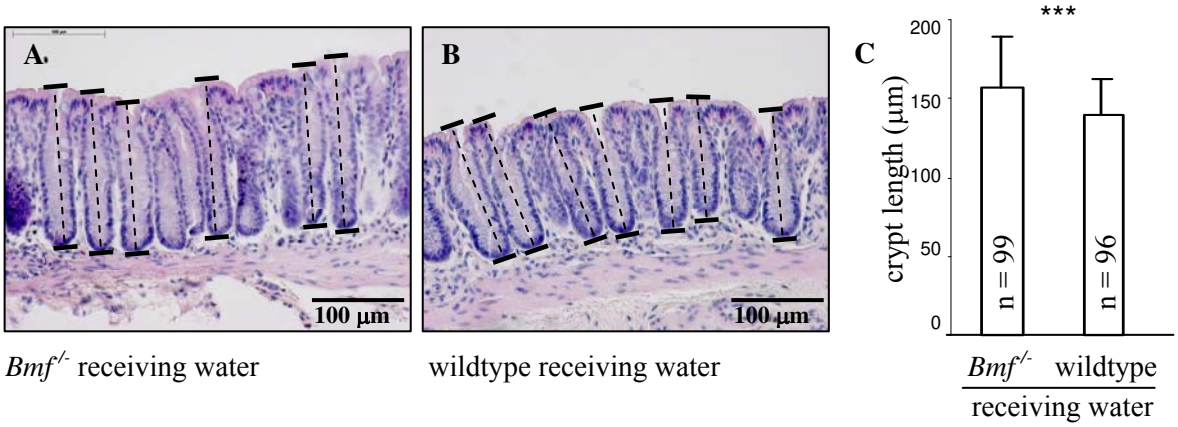


*Bmf*$^{-/-}$ receiving water wildtype receiving water

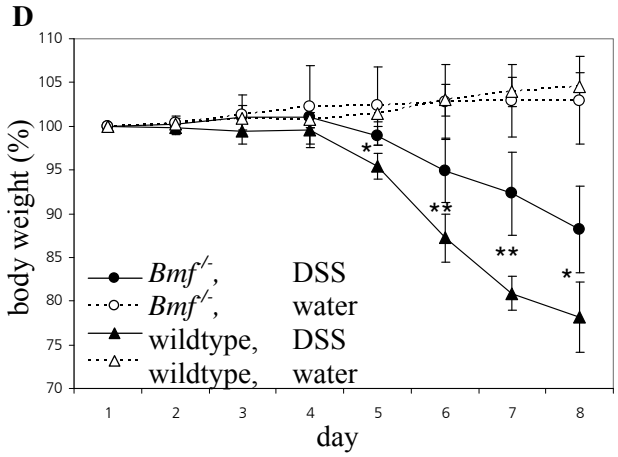

**Figure 2**

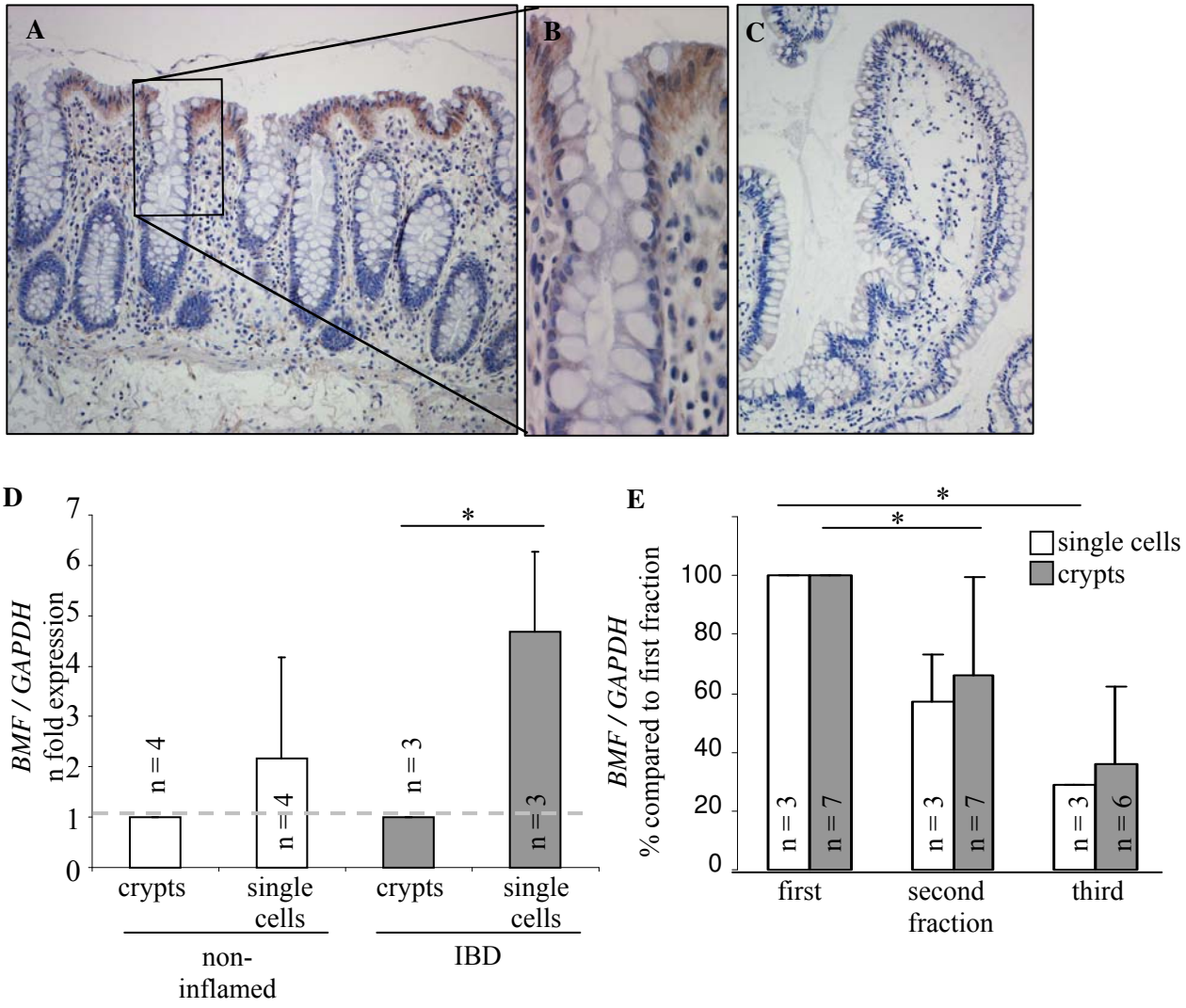
A
B
C
D
BMF / GAPDH
n fold expression
0
1
2
3
4
5
6
7
*
n = 4
n = 4
n = 3
n = 3
crypts
single cells
crypts
single cells
non-inflamed
IBD
E
BMF / GAPDH
% compared to first fraction
0
20
40
60
80
100
*
*
single cells
crypts
n = 3
n = 7
n = 3
n = 7
n = 3
n = 6
first
second fraction
third

**Figure 3**

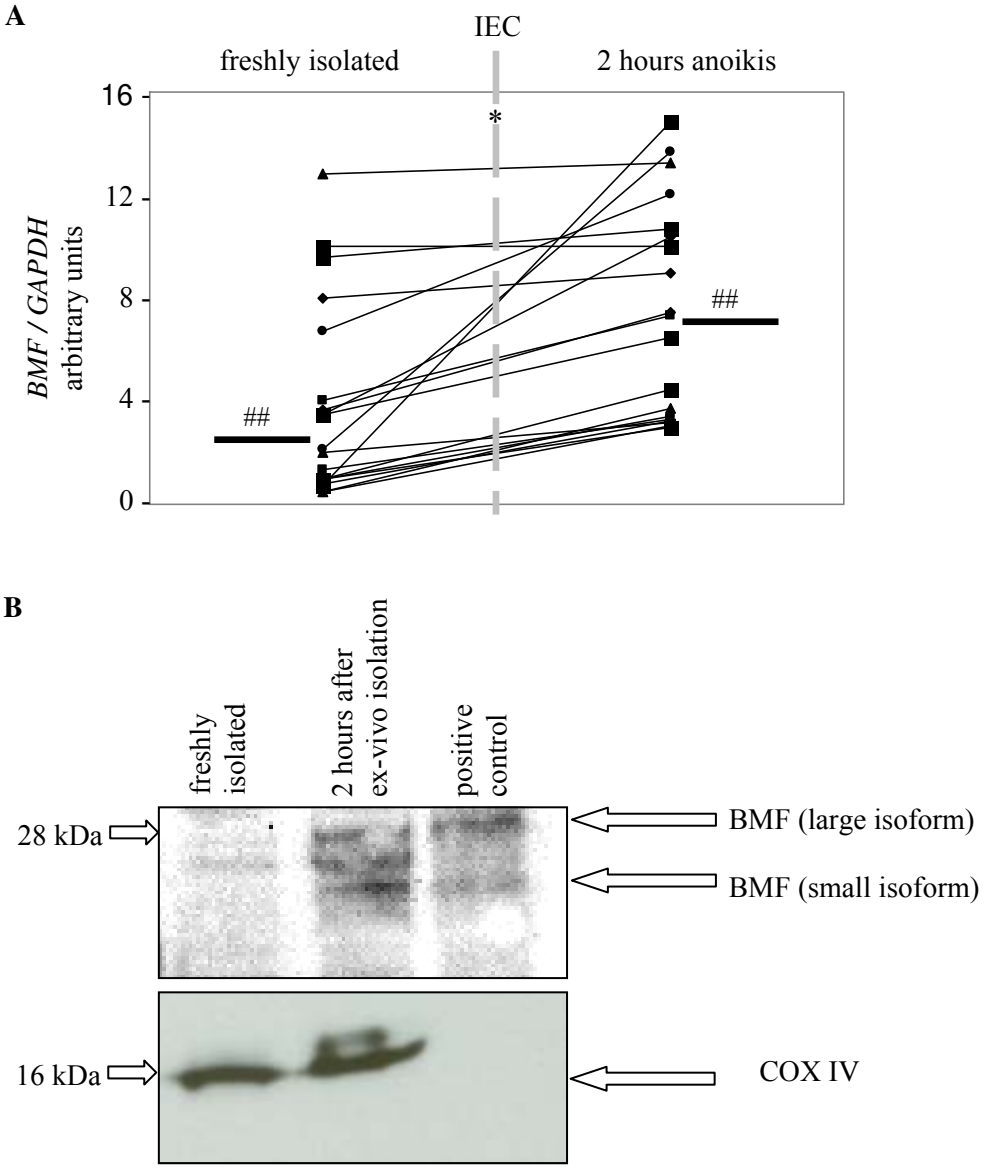
A
IEC
freshly isolated
2 hours anoikis
16
12
8
4
0
*
##
##
BMF / GAPDH
arbitrary units
B
freshly isolated
2 hours after ex-vivo isolation
positive control
28 kDa
BMF (large isoform)
BMF (small isoform)
16 kDa
COX IV

**Figure 4**

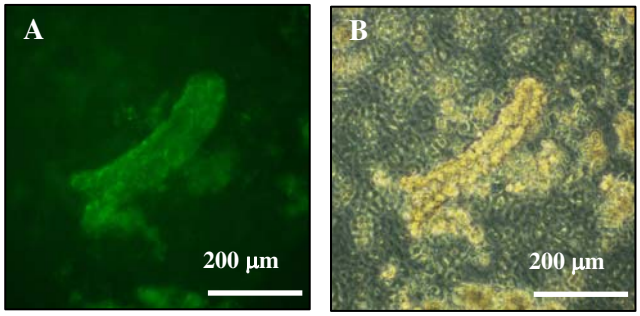
A
200 µm
B
200 µm

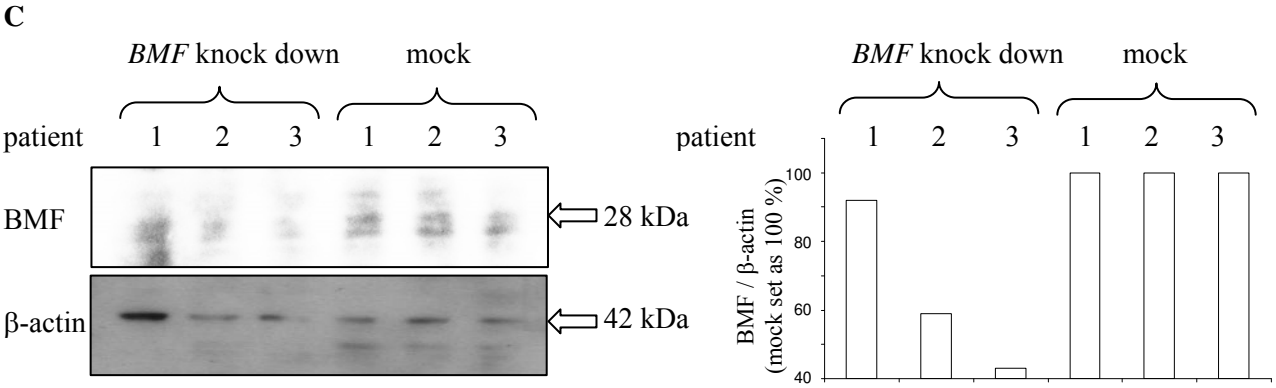
C
BMF knock down
mock
patient
1 2 3 1 2 3
BMF
28 kDa
β-actin
42 kDa
BMF knock down
mock
patient
1 2 3 1 2 3
BMF / β-actin
(mock set as 100 %)
100
80
60
40

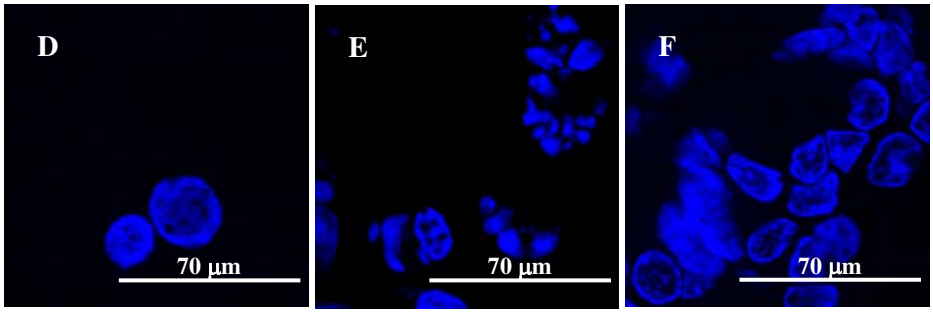
D
70 µm
E
70 µm
F
70 µm

**Figure 5**

**A**

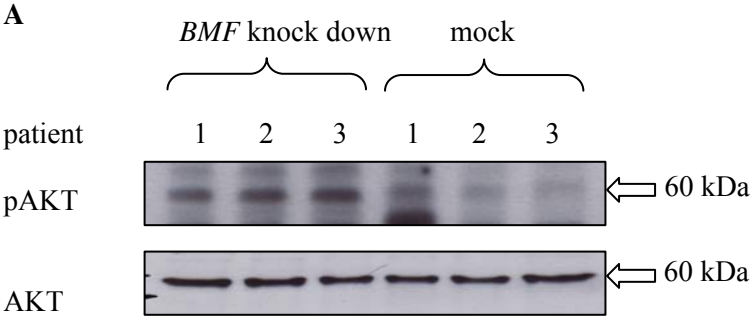


**B**

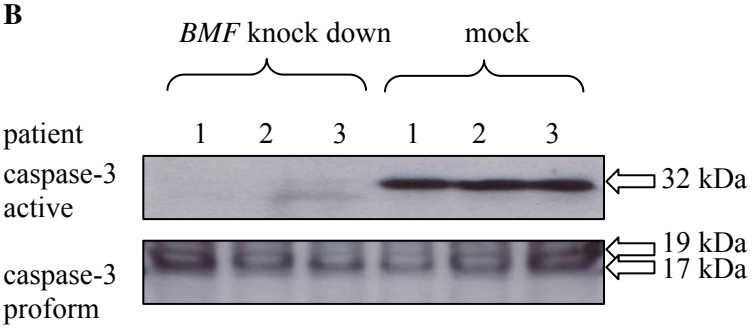


**C**

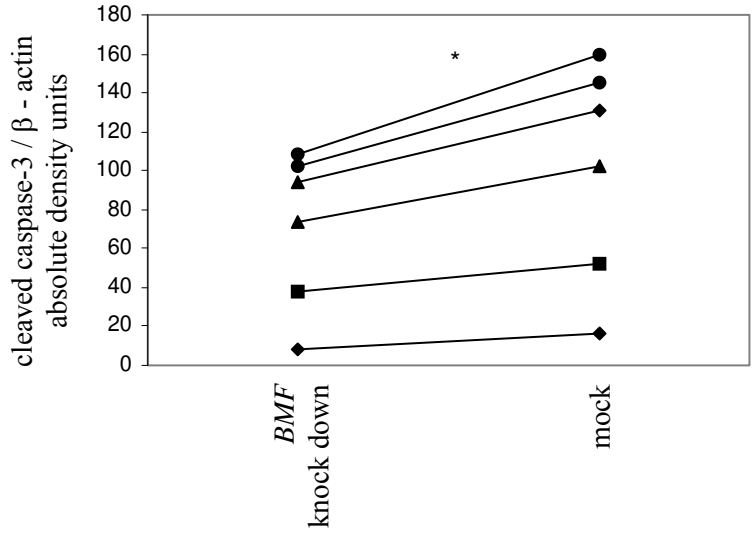


**D**

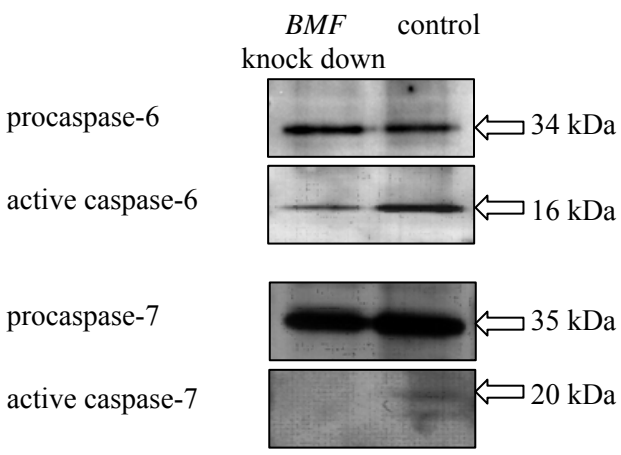

**E**

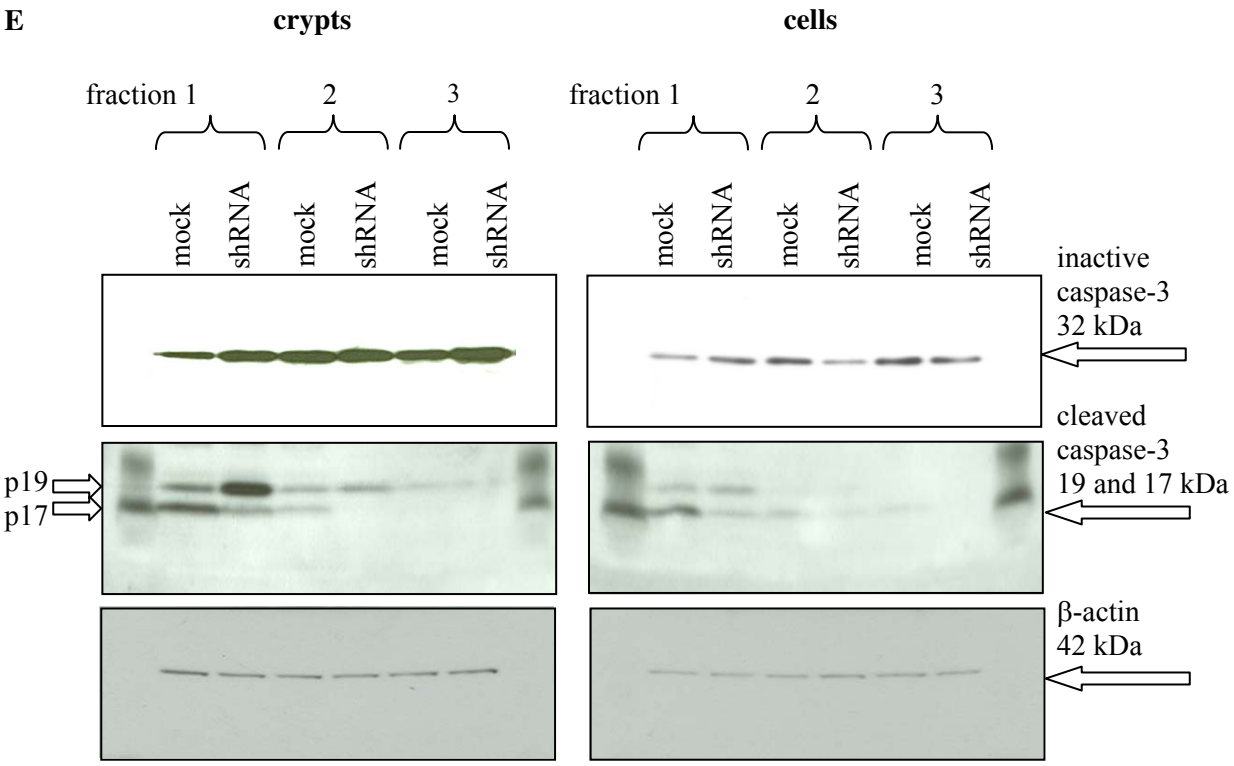
crypts
cells
fraction 1
2
3
mock
shRNA
inactive
caspase-3
32 kDa
cleaved
caspase-3
19 and 17 kDa
p19
p17
β-actin
42 kDa